

Conducted high frequency disturbances observed in electrical power systems with switch mode converters

Abstract. This paper deals with electrical power systems (EPS) with power electronics interfaces. The EPS with switch mode converters (SMC) are of particular interest. In general, one of the phenomena of SMC topologies is the generation of signal perturbation and examples of such signal perturbation from test results are presented. A simplified equivalent circuit model of the common mode (CM) and differential mode (DM) voltage and current analysis in a three-phase system is introduced. Furthermore, many examples of experimental test results in EPS with SMC are presented.

Streszczenie. Artykuł dotyczy systemów elektroenergetycznych (SE) z interfejsami energoelektronicznymi. Szczególnie są to SE z przekształtnikami energoelektronicznymi (PE) o sterowaniu typu PWM. W ujęciu ogólnym, przedstawiono wyniki badań sygnałów zaburzeń, które są efektem stosowania PE w tych systemach. Wprowadzono model obwodowy systemu trójfazowego do analizy zaburzeń napięć i prądów typu CM oraz DM. Ponadto, przedstawiono wiele przykładowych wyników badań eksperymentalnych zaburzeń w SE z PE. (Zaburzenia przewodzone wysokiej częstotliwości obserwowane w systemach elektroenergetycznych z przekształtnikami energoelektronicznymi o sterowaniu typu PWM).

Keywords: electrical power system, switch mode converter, compensator, conducted electromagnetic interference.

Słowa kluczowe: system elektroenergetyczny, przekształtnik energoelektroniczny o sterowaniu typu PWM, kompensator, zaburzenia elektromagnetyczne.

Introduction

Electrical power systems are very important and convenient ways to “keep alive” industrial and social systems. These systems can be divided into electrical energy transmission systems (EETS) and electrical energy distribution systems (EEDS) [1]-[11]. In EETS there are two technologies used for controlling the transmission of energy: (i) high, medium or low voltage direct current (HVDC, MVDC, LVDC) devices with DC transmission and (ii) flexible alternating current transmission system (FACTS) devices, (Fig. 1) [5], [8]. In EEDS there are also two technologies used for controlling the transmission of energy: (i) coupling of renewable or stored distributed electrical energy sources with EPS or local end-user and (ii) interfacing passive and active load or local end-user in order to supply quality improvement, (Fig.2) [6]-[9].

All types of the electrical energy conversion are used in EPS which are realized by AC/DC, DC/AC, DC/DC and AC/AC power electronics converters [6], [11]-[13]. Increasingly, there are switch mode converters with self commutated switches (transistors) in such circuits. Even for high power converters (a few MVA) using transistor switches based on insulated gate bipolar transistors (IGBT), rise or fall time of the voltages or currents are smaller than a few microseconds [14]. This produces rates of du/dt and di/dt with values even more than $1\text{ kV}/\mu\text{s}$ or $1\text{ kA}/\mu\text{s}$ respectively. It leads to many EMC related side effects [11], [15], [16].

A typical approach to electromagnetic emission measurements is based on the use of standardized equipment and comparison of the result obtained in normalized arrangement with specific limit lines related to EUT (Equipment Under Test). In this case, classical filter development is limited to the selection of a device with a desired attenuation in a given frequency range [17, 18]. However, evaluation of the electromagnetic compatibility in defined (not EMC standard) context and the development of effective disturbance mitigating techniques [19]-[21] require knowledge of specific phenomena accompanying the application of SMC in electrical power systems.

The aim of the paper is to present recent results, obtained by the authors [22]-[27], concerning generation and flow of disturbances introduced into electrical power systems by switch mode converters.

Switch mode converters

In Electrical Energy Transmission Systems

The types of electrical energy conversion in EETS are shown in Fig. 1. In general, in HV-, MV- and LVDC transmission systems AC/DC and DC/AC converters are used, whereas in FACTS different types of converters, including also AC/AC with and without DC storage, are applied.

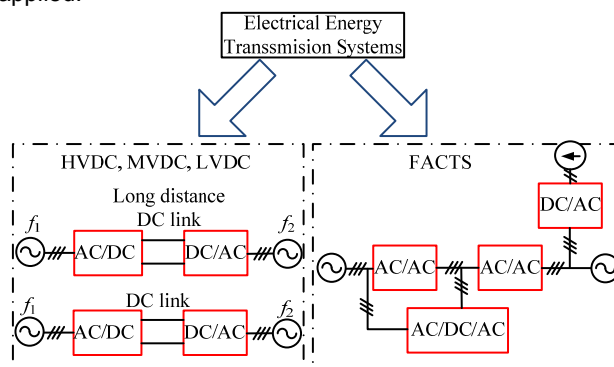


Fig. 1. Electrical energy transmission systems

In Electrical Energy Distribution Systems

Types of electrical energy conversion in EETS are shown in Fig. 2. In general, in coupling renewable or storage distributed electrical energy sources with EPS or local end-users DC/AC converters are used for the voltage or current profiling of DC sources, e.g., photovoltaic cells, whereas AC/AC indirect or direct converters are used for the voltage or current profiling of AC sources e.g., wind turbine generator. There are similar types of power electronics converters in interfacing EPS with passive loads e.g., electro thermal actuators or active loads e.g., DC or AC drive systems.

LVDC or AC/DC/AC Converter

An example of the LVDC or AC/DC/AC topology is shown in Fig. 3 [11], [15], [14]. In this circuit two switch mode converters are used. Both are used as the rectifier and the inverter for the energy flow from line-side source to output side source or inversely. In general, each converter has 8 allowed switch configurations and control strategies, usually with space vector modulation (Fig. 3b), being used [28]. Multilevel converters are also applied, inter alia, because of

the du/dt lowering ratio. An example of the five level converter with cascade H-bridge topology is shown in Fig. 4 [28], [29].

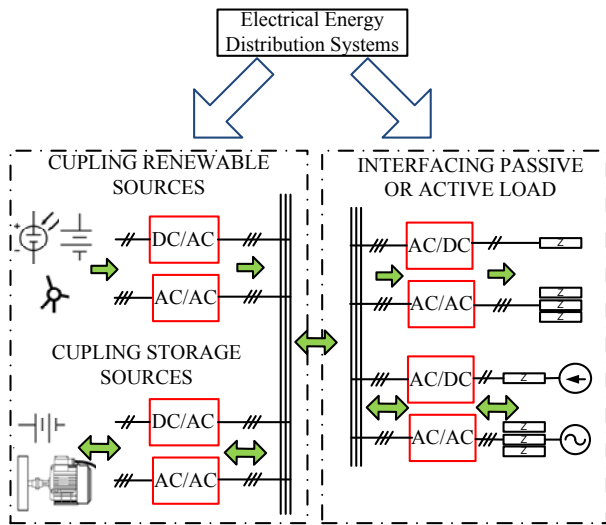


Fig. 2. Electrical energy distribution systems

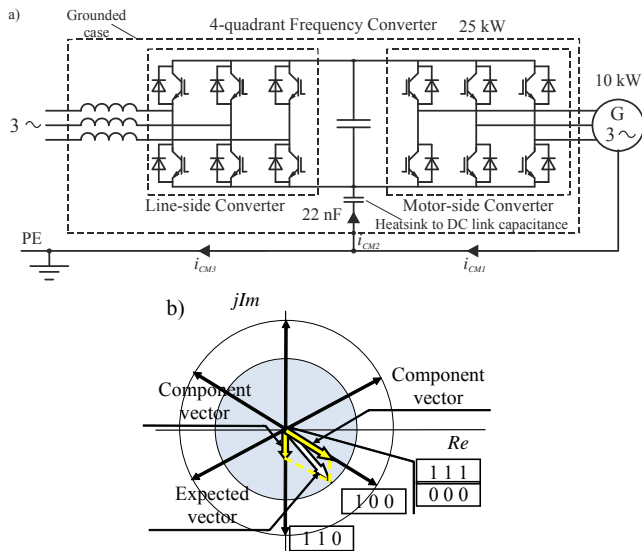


Fig. 3. AC/DC/AC frequency converter in drive system, a) 4-quadrant topology, b) simplified geometrical interpretation of the space vector synthesis

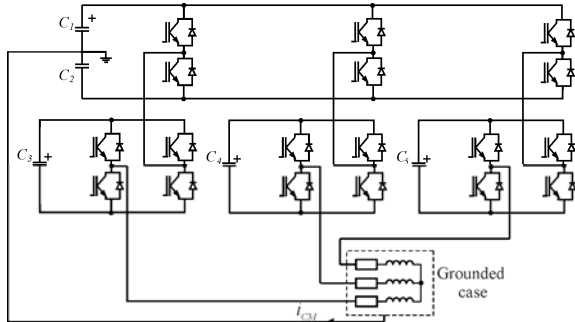


Fig. 4. Five level cascaded H-bridge inverter

Unified Power flow Controller

An example of the UPFC, the most universal power electronics device of the FACTS, is shown in Fig. 5 [29], [30]. Two voltage source inverters (VSI) are used as the compensation voltage u_c and as the compensation current i_c sources.

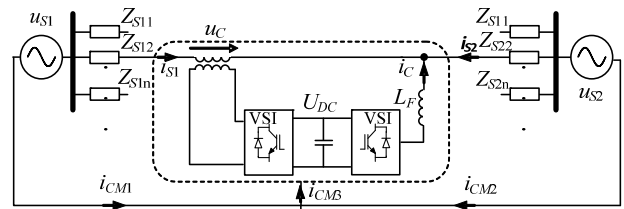


Fig. 5. UPFC in AC/AC transmission system

DC/DC Converter

An example of the DC/DC converter with Z-source interface and high frequency step-up insulation transformer is shown in Fig. 6 [11]. Usually, the PWM H-bridge bipolar inverter and voltage doubler rectifier are used.

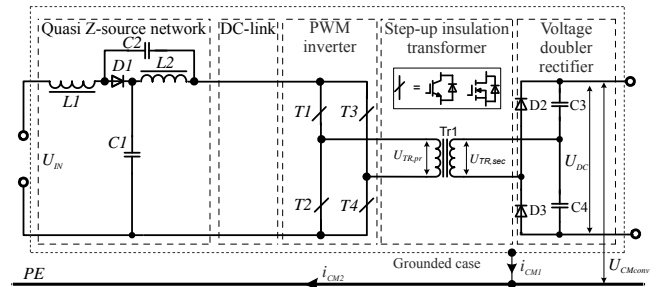


Fig. 6. DC/DC converter with high frequency insulated transformer

AC/DC Converter

A three-phase PWM rectifier cascade connected with a buck topology DC/DC converter for bidirectional power flow control to or from a battery, exemplifying the distribution system, is shown in Fig. 7 [11].

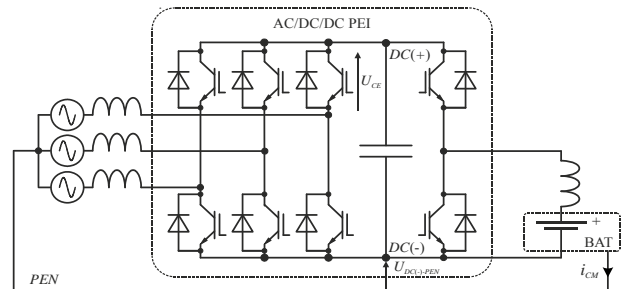


Fig. 7. AC/DC converter in distribution system with active load

Theoretical Base

General Description

Fig. 8 schematically shows intentional and parasitic electromagnetic processes in systems containing power electronic converters [15]. For the most commonly encountered system operation conditions (resistive-inductive load, pulse width modulation and switching frequencies of a few kHz) it is possible to predict certain characteristic EMI (Electromagnetic Interferences) currents:

- the carrier frequency and its harmonics are predominant in the EMI current spectrum in the lower (CISPR A) EMC frequency band,
- EMI currents excited by fast du/dt in parasitic resonant circuits prevail in CISPR B frequency range,
- because of their origin EMI currents in CISPR B frequency range will have approximately damped oscillatory waveforms with frequencies not exceeding 30 MHz (upper limit of conducted EMI),
- the near square waveforms of voltage excitation and large extent of systems causes the wave approach to be very useful in analyses.

In order to describe EMI current paths and the appropriate application of emission reduction techniques the method of splitting EMI current into a Common Mode (CM) and a Differential Mode (DM) is commonly used. CM noise is a type of EMI induced on signals with respect to a reference ground. The remainder of the total conducted EMI

is defined as the DM noise. The CM/DM current paths in three-phase systems for step excitation in the phase B are shown in Fig. 9. Lumped RLC elements represent parasitic and residual parameters (of source, cable and load respectively) of EMI noise paths.

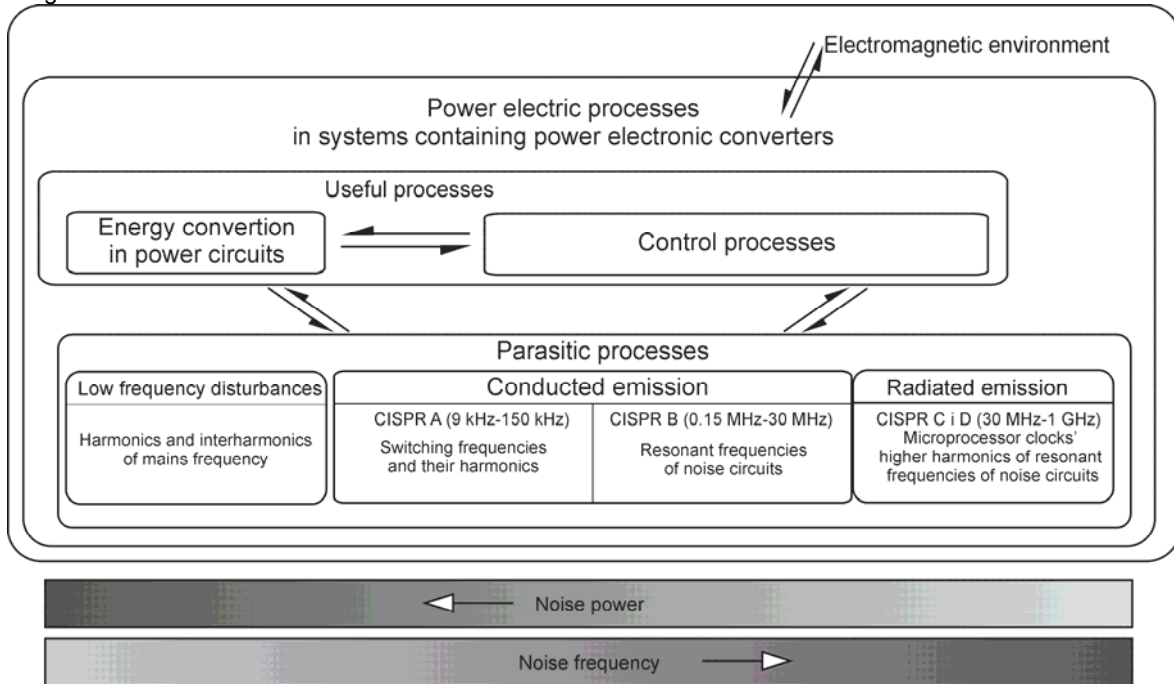


Fig. 8. Intentional and parasitic electromagnetic processes in systems with power electronic converters

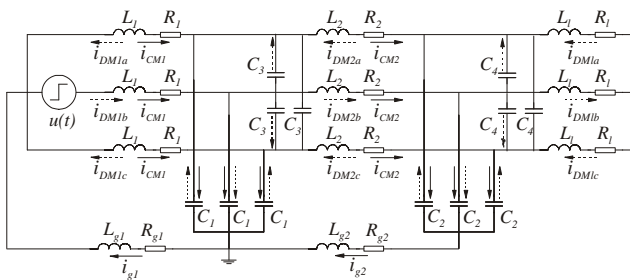


Fig. 9. The CM/DM current paths in three-phase systems for step excitation in the phase B

EMI currents in HF CISPR B range

EMI currents spread over systems in complex circuits containing parasitic parameters (that are in fact distributed). While the CM/DM separation is well defined and understood for the single-phase or the DC system, the same cannot be said of three-phase converter systems and there is no universal CM/DM definition [31]. However, splitting three-phase-systems into CM/DM is still possible if a symmetrical, linear and time invariant three phase system is considered. In CISPR B frequency range, using some orthogonal transformations (e.g. $\gamma, \delta, 0$) and the Laplace transform it is possible to transform the three-phase circuit of fig. 9 which contains parasitic elements into to the single-phase CM and DM circuits shown in Fig. 10 [15].

It is usually possible to separate dominant oscillation mode in CM and DM current waveforms. This allows the adoption of a simple RLC model, and in normal practice this is the basis for analyses and the selection of EMI mitigating techniques. In regard to the pulse nature of voltages in power electronic converters the step function is often used in simplified analyses as an excitation in EMI current circuits. However, the trapezoidal function fits better with experimental voltage waveform because although the

frequency of the oscillation in a circuit with trapezoidal excitation depends on parameters of passive elements, the resulting shape and maximum value of the current are strongly influenced by rise and fall times of the voltage slope. For convenience of analysis the leading edge of a trapezoidal signal can be split into two linear excitations, as shown in Fig. 11.

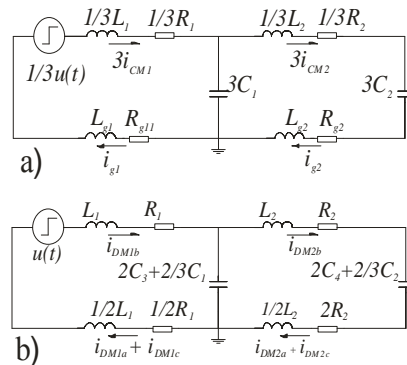


Fig. 10. Single-phase substitute schemes: a) for CM, b) for DM

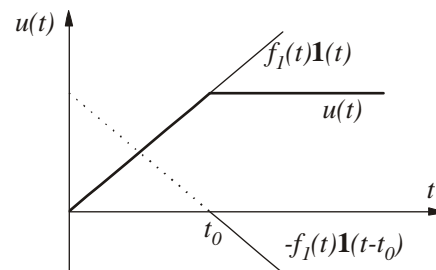


Fig. 11. Graphical interpretation of the voltage step function

Time varying voltage $u(t)$ can be expressed by (1),

$$(1) \quad u(t) = \frac{\Delta U}{t_0} t \cdot \mathbf{1}(t) - \frac{\Delta U}{t_0} (t - t_0) \cdot \mathbf{1}(t - t_0),$$

where: ΔU - voltage step, $\mathbf{1}(t)$ - unit step function, t_0 - rise time.

Using Laplace transform theory the waveform of the current in a series RLC circuit can be expressed by (2),

$$(2) \quad i(t) = \frac{\Delta U}{t_0} \frac{1}{L} [K\mathbf{1}(t) - Ae^{-\alpha t} \sin(\omega_0 t + \beta)] \mathbf{1}(t) - K\mathbf{1}(t - t_0) - Ae^{-\alpha(t-t_0)} \sin[\omega_0(t-t_0) + \beta] \mathbf{1}(t - t_0)$$

where: $\omega_0^2 = \omega_n^2 - \alpha^2 = \frac{1}{LC} - \frac{R^2}{4L^2}$, R, L, C - resulting resistance, inductance and capacitance of the circuit, $\alpha = R/2L$ - damping factor

$$A = \frac{1}{\omega_0} \frac{1}{\sqrt{\alpha^2 + \omega_0^2}}, \quad K = \frac{1}{\alpha^2 + \omega_0^2}, \quad \beta = \arctan \frac{\omega_0}{\alpha}.$$

The current responses of a series RLC circuit to excitation with different rise times t_0 and the spectra of these currents are shown in Fig. 12.

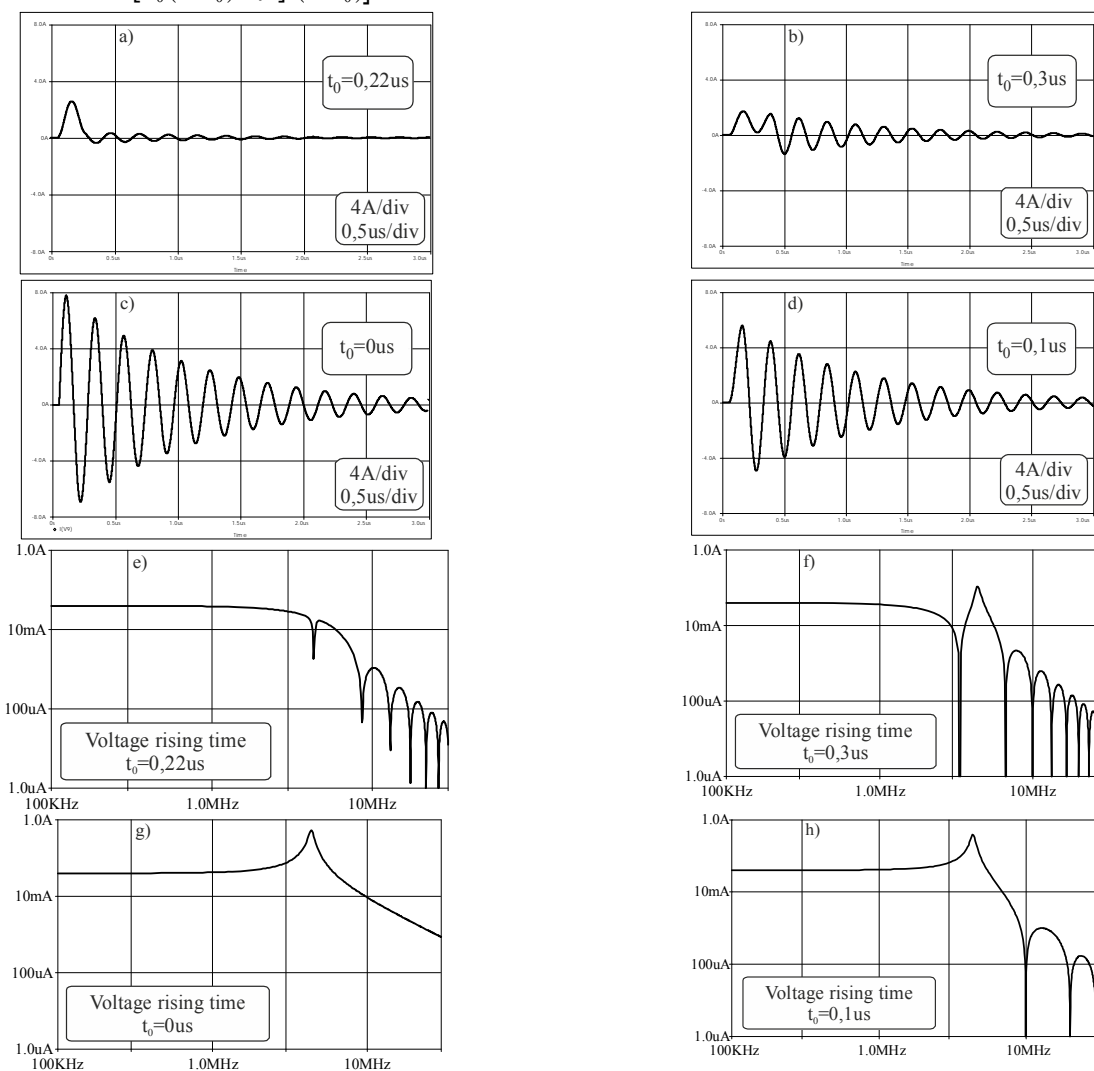


Fig. 12. Time waveforms and spectra of the current responses for different rise times, a), b), c), d) time waveforms, e), f), g), h) spectra of currents

Generally, currents have damped oscillatory waveforms, however for the specific rise time of voltage ($t_0 = 1/f$ where f is resonant frequency of the circuit) there has been observed strong attenuation of ringing. This is very important because the lack of a characteristic peak in the EMI current spectrum can lead to misinterpretation of experimental data. It is worth noting that there is a strong dependence of the current amplitude on the voltage rise time. The ringing phenomena can exacerbate the problems of EMI, overvoltages and signal integrity in systems containing power electronic converters. Additionally, the ringing transients cannot fully decay prior to the occurrence

of the next pulse that can cause ringing higher than in the case of a single pulse (double pulsing).

Analytical decomposition of phase voltages in CISPR A frequency band

Usually, EMI noises connected with control algorithms of PWM drive systems are located in CISPR A band because of typically used carrier frequencies in such systems [28]. To determine voltage excitations for both modes the double Fourier integral analysis may be applied. Three-phase naturally sampled (sinusoidal) PWM will be used as an example of decomposition. For this algorithm phase voltages can be expressed by the well known expression (3) [4].

$$\begin{aligned}
u_{iN}(t) &= V_{DC} + V_{DC}M \cos(\omega_0 t + \theta_i) + \\
&\frac{4V_{DC}}{\pi} \sum_{m=1}^{\infty} \frac{1}{m} J_0\left(m \frac{\pi}{2M}\right) \sin\left([m+n]\frac{\pi}{2}\right) \times \\
(3) \quad &\times \cos(m\omega_c t + n[\omega_0 t + \theta_i]) + \\
&\frac{4V_{DC}}{\pi} \sum_{m=1}^{\infty} \sum_{n=-\infty}^{\infty} \frac{1}{m} J_n\left(m \frac{\pi}{2} M\right) \sin\left([m+n]\frac{\pi}{2}\right) \times \\
&\times \cos(m\omega_c + n[\omega_0 t + \theta_i])
\end{aligned}$$

where: $i = a, b, c$ -phase leg identifiers for three phase inverter, m, n -harmonic index variables, V_{DC} -one-half of DC-link voltage, $J_n(x)$ -Bessel function of order n and argument x , ω_c -angular frequency of carrier waveform, ω_0 -angular frequency of fundamental component, M - modulation index.

The theoretical harmonic spectra of the phase voltage for a three-phase natural sampled (sinusoidal) PWM as a function of the modulation index is shown in Fig. 13. The common mode voltage source is expressed by (4).

$$(4) \quad u_{CM}(t) = \frac{u_a(t) + u_b(t) + u_c(t)}{3},$$

where: u_a, u_b, u_c -phase voltages.

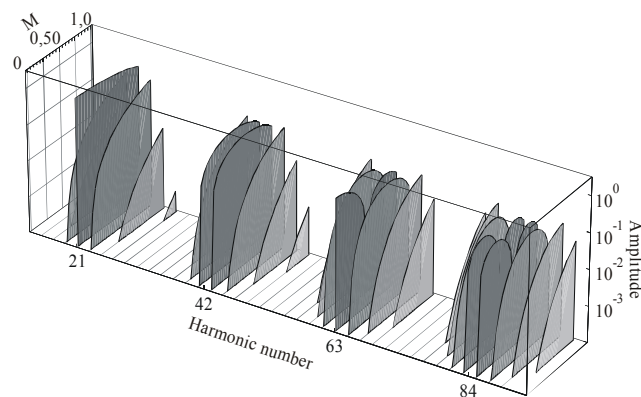


Fig. 13. Normalized harmonic spectra of the phase voltage

Sideband harmonics with even combination of $m \pm n$ will not appear in this sum because of the term $\sin\left([m+n]\frac{\pi}{2}\right)$. The elimination term $\cos\left[1 + 2\cos\left(n \cdot \frac{2\pi}{3}\right)\right]$ causes a cancellation of specific harmonics in the CM voltage. Harmonics, which are cancelled in the CM voltage, are represented in the DM voltage because of the term $\sin n\pi/3$. Using the above mentioned terms, common and differential mode components in phase voltages can be expressed as in (5) and (6).

$$\begin{aligned}
(5) \quad u_{DMi}(t) &= \frac{8V_{DC}}{\sqrt{3}\pi} \sum_{m=1}^{\infty} \sum_{n=-\infty}^{\infty} \frac{1}{m} J_n\left(m \frac{\pi}{2} M\right) \sin\left([m+n]\frac{\pi}{2}\right) \times \\
&\times \sin n \frac{\pi}{3} \cos(m\omega_c t + n\omega_0 t)
\end{aligned}$$

$$\begin{aligned}
(6) \quad u_{CM}(t) &= \frac{4V_{DC}}{3\pi} \sum_{m=1}^{\infty} \sum_{\substack{n=-\infty \\ n \neq 0}}^{\infty} \frac{1}{m} J_n\left(m \frac{\pi}{2} M\right) \times \\
&\times \sin\left([m+n]\frac{\pi}{2}\right) \left[1 + 2\cos n \frac{2\pi}{3}\right] \times \cos(m\omega_c t + n\omega_0 t)
\end{aligned}$$

The result of the analytical decomposition of the phase voltages into CM and DM components for arbitrarily selected parameters of the modulation (modulation index $M = 0.9$, $f_c / f_o = 21$) are shown in Fig. 14.

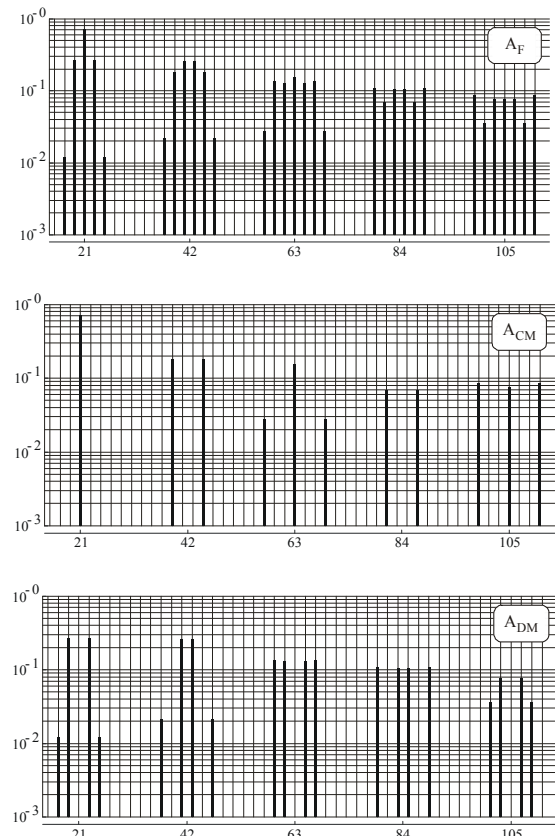


Fig. 14. Spectra, a) phase voltage, b) CM voltage component and c) DM voltage component

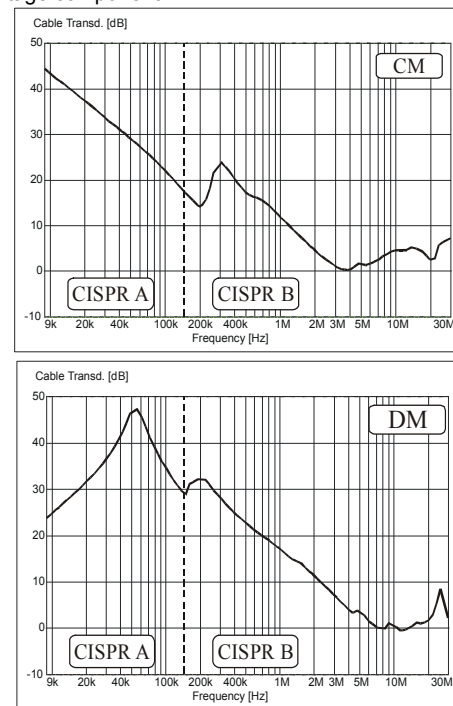


Fig. 15. Insertion losses of CM and DM paths on the motor side of the drive system

In order to determine the current harmonics, advantage can be taken of the fact in CISPR A frequency band the impedance of the common mode path is predominantly

capacitive in character. As an example, Fig 15 shows the insertion losses of CM and DM paths on the motor side of the drive system (Fig. 15).

After taking into account the impact of the measuring range of the receiver on the result, we can enter the distribution of computational normalized harmonic common mode currents A_{mn}'' , weighted by the number of harmonic group (m) and aggregated around the harmonic output frequency according to the formula (7) [15], [32].

$$(7) \quad A_{mn}''(\omega) = \sum_{n=-\infty}^{n=\infty} A_{mn}(\omega) \cdot m.$$

In Fig. 16 are shown the spectrum obtained this way for modulation indexes $M = 0.9$ and $M = 0$.

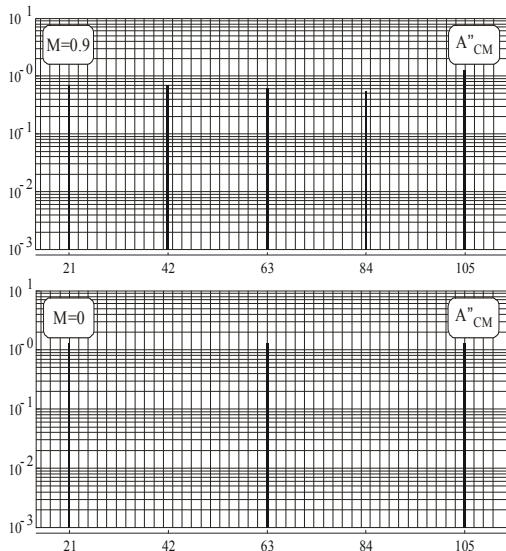


Fig. 16. Spectrum of weighted and aggregated harmonics of CM voltage

Travelling wave phenomena

On account of high du/dt at the output of the inverter, EMI currents in the motor cable are, in fact, travelling wave phenomena in feeder cables and motor windings [15], [33], [34]. The understanding of these phenomena is very important for a proper analysis of EMI spectra. An exemplification of the effect of travelling wave phenomena on CM and DM noise spectra is shown in Fig. 17. Travelling waves have been excited in a shielded and unshielded open-ended cable fed by an inverter. The velocity of the electromagnetic waves can be approximately expressed by (8)

$$(8) \quad v = \frac{1}{\sqrt{\epsilon_0 \epsilon_r \mu_0 \mu_r}},$$

where: ϵ_0 is the dielectric constant, ϵ_r is relative permittivity, μ_0 is the permeability of the free space, μ_r is relative permeability.

The frequency of the noise is formed by multiple reflections of the travelling wave and depends on the propagation time between reflections. The circuits of CM and DM currents can be quite different. However, in the case of the shielded cable, the frequencies of the main oscillatory modes are approximately the same, because electromagnetic waves propagate in the material with similar permittivity.

For the unshielded cable, the electromagnetic wave connected with DM noise propagates in the solid material as in the case of a shielded cable. Therefore, the spectrum

of EMI noise remains unchanged. Otherwise, the electromagnetic wave that constitutes the CM leakage current propagates mainly in the air, which results in an increased wave velocity. This in turn causes a higher frequency of the main oscillation mode. The magnitude of CM spectra is much smaller because of decreased transverse line-to-ground parasitic capacitances. The observations made on the basis of the above-presented spectra have been confirmed by measurements in time. The waveforms of phase voltage, phase current, DM and CM noise currents are shown in Fig. 18.

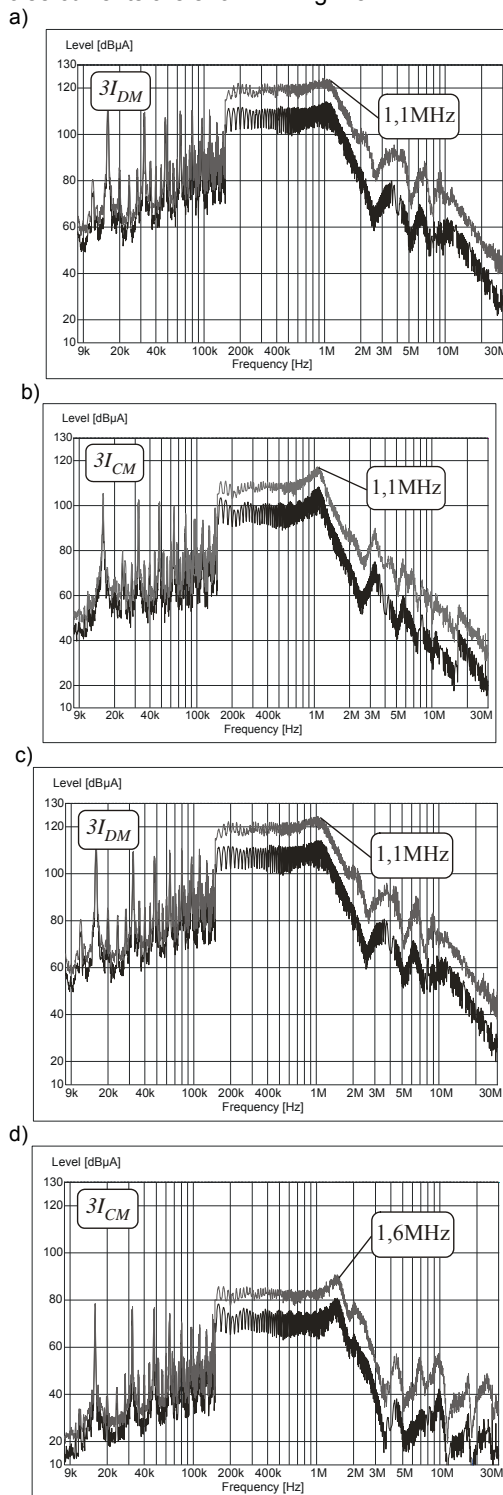


Fig. 17. EMI currents spectra in: a), b) shielded and c), d) unshielded cable

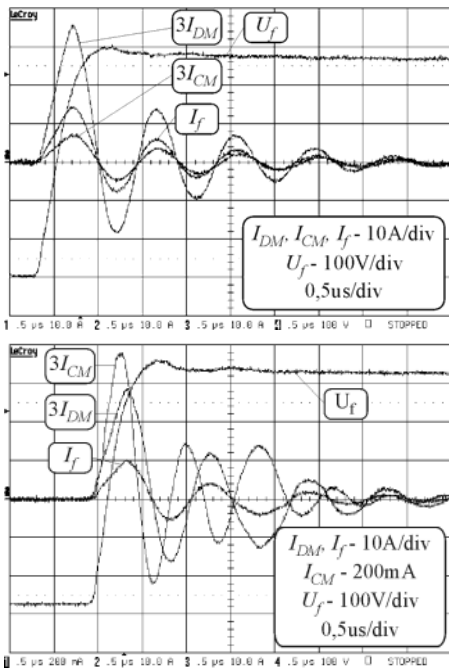


Fig. 18. Voltage, phase current, DM and CM noise currents in a shielded and unshielded cable

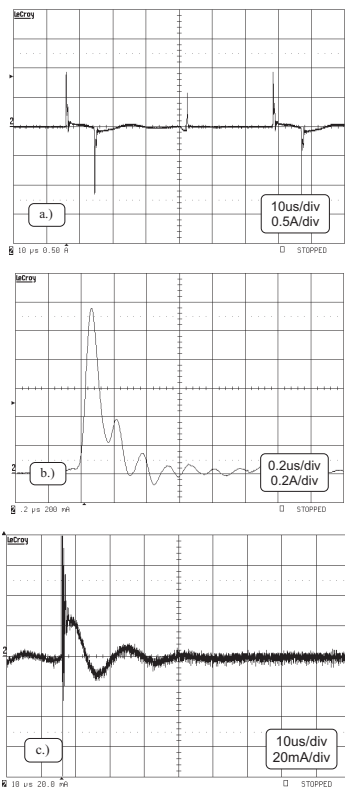


Fig. 19. a) Common mode current in motor PE wire, b) HF component of CM current, c) LF oscillatory of CM current

Experimental Test Results

Conducted EMI generated by two-quadrant frequency converter

CM currents, which are generated by switching states of the inverter, have an impulse-like waveform with HF oscillation. The resonant frequency of the oscillatory mode is determined by the residual, parasitic parameters of the CM current path. Fig. 19 shows the main oscillatory modes of the CM current, generated by the 7.5 kW two-quadrant frequency converter, supplying the 1.5 kW induction motor.

The main return path for the CM currents leads through the heat sink to DC link capacitance. The CM current causes a CM voltage drop in the heatsink-to-DC link capacitance. In the blocking state of the rectifier diodes, only the higher frequency part (oscillatory modes of approximately 160 kHz and 6.8 MHz) of this current flows through the series parasitic capacitance of the diode and converter supply arrangement. In the conduction state, the voltage drop in the heatsink-to-DC link capacitance causes oscillation of the relatively low frequency (approximately 16 kHz) in the shape of CM current that flows in a closed loop consisting of a DC-link-to-heatsink capacitance, the resultant inductance of the mains (or LISN), the cable and the input filter [35, 36]. The CM current (i_{CM}) and phase current (i_p) on the line side of the converter in the conduction and blocking states of the rectifier diodes are shown in Fig. 20.

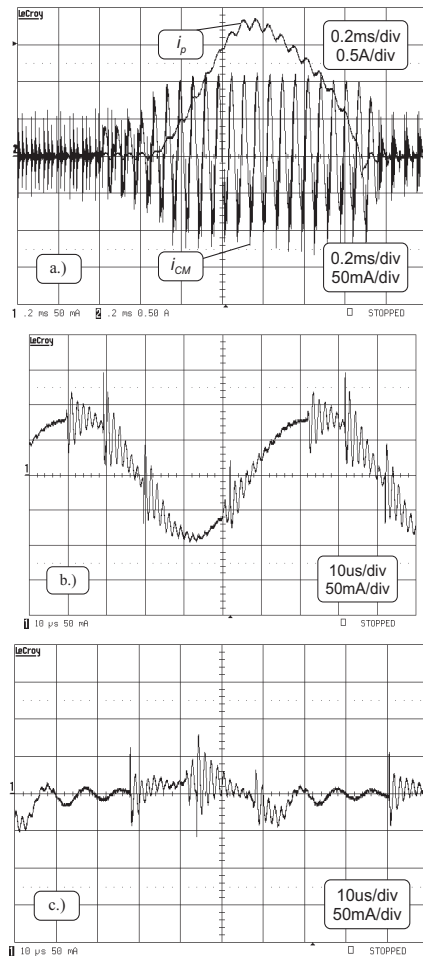


Fig. 20. a) CM current on the line side of the converter and rectifier phase current, b) CM current in conduction state of the rectifier, c) CM current in blocking state of the rectifier

Conducted EMI generated by four-quadrant frequency converter

The experimental results presented in previously published papers indicated that there are two CM voltage sources in a four-quadrant AC drive system; one on the line side of the converter and a second one on the motor side [22], [24].

The measurements in the time domain have been made in the system presented in Fig. 3 consisting of a 25 kW four-quadrant frequency converter and a 10 kW induction motor. Fig. 21 shows the CM currents measured on both sides of the converter.

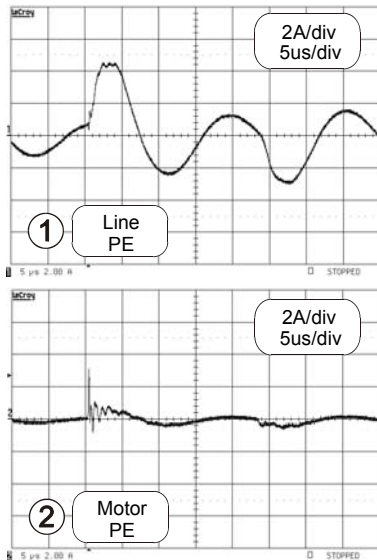


Fig. 21. Passage of common mode currents through “grounding point”

Flows of CM interferences generated by a four-quadrant frequency converter in LV and MV grid

In order to evaluate the depth of interference penetration into the electric grid measurements in LV and MV grids were performed [26], [36]. The converter shown in Fig. 3 was connected directly to the mains without a LISN (Line Impedance Stabilization Network). The result of CM current measurement in CISPR A frequency band, using peak (upper line) and average (lower line) detectors, is shown in Fig. 22. The main frequency modes (S&H clock frequency 40 kHz, and envelope of spectra typical for damped oscillatory mode of 70 kHz) observed in the spectrum are related to those in the time domain presented in Fig.21.

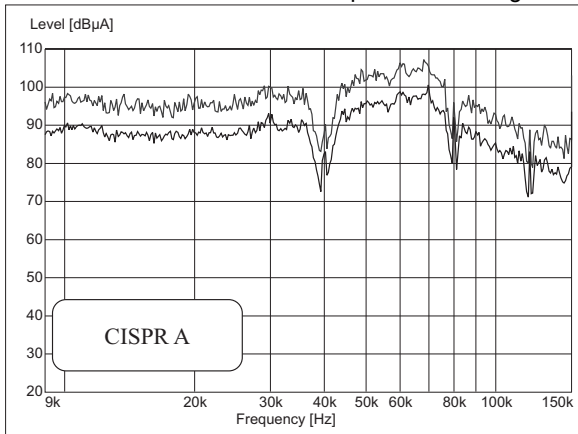


Fig. 22. Spectrum of CM current in converter PE wire

Fig. 23 shows the results of magnetic field strength measurements in the power transformer on both low and medium voltage sides.

The need to carry out research on conducted electromagnetic interference in medium voltage (MV) grids forced the application of the field measuring method. The active loop antenna was used for measuring interference penetration depth into the MV grid. The investigations were carried out at an urban type transformer station. The generator and converter were connected to the LV side of the 160 kVA transformer.

The presented experimental results show that interference introduced by the converter is transferred by parasitic capacitive couplings onto the MV side of the transformer (not synchronized to the transformer ratio). In

this case the transformer cannot be treated as an attenuating device for high frequency interference.

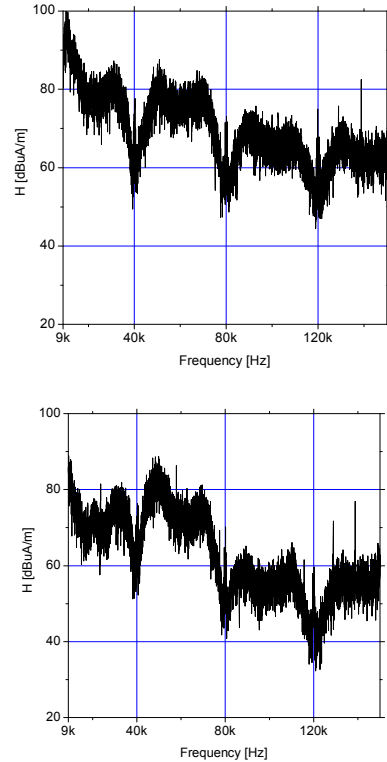


Fig. 23. Magnetic field strength on both sides of power transformer: a) low voltage side, b) medium voltage side.

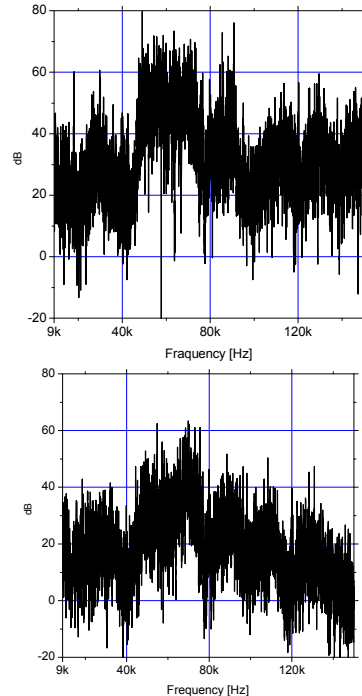


Fig. 24. Increase of interferences caused by converter under MV overhead lines: a) 20 m away from station, b) 1300 m away from station

Further investigations were performed under overhead MV lines. The first measurement was taken 20 m away from the transformer station. The second measuring point was located under an overhead MV line 1300 m away from the transformer station. In both cases the loop antenna was oriented along the lines in order to assure maximum level of interference measured in the near field.

Fig. 24 shows an increase of interference caused by the converter in comparison with background interference under MV overhead lines 20 m and 1300 m away from the transformer station.

The presented results show that four-quadrant converters, generating a high level of conducted EMI, connected to the LV grid may cause a 40-60dB increase in interference at distant points under MV lines. For characteristic, oscillatory mode frequencies introduced by the converter, the observed attenuation amounted to 10-20dB for these two points. It is important to note that due to the above described travelling wave, especially standing wave, phenomena the measured attenuations should be treated as approximate levels and might change along the line.

CM voltage produced by DC/DC converters

DC/DC converters supply a DC voltage generated in a differential mode (DM) circuit consisting in a bulk capacitor. However, plus and minus DC bus potentials with respect to ground change their values. Fig. 25 shows DC voltage at the output of the converter (U_{DC}), plus DC-to-ground voltage ripples (U_{+DC}) and minus DC-to-ground voltage ripples (U_{-DC}). The observed fast changes of the plus and minus DC voltage buses with respect to ground bring about common mode (CM) current flow in the presence of a CM capacitance on the load side of the DC/DC converter. In practice, it is usually parasitic to ground capacitance of the load or capacitance of the Y-type capacitors dedicated to the CM circuits of EMI filters.

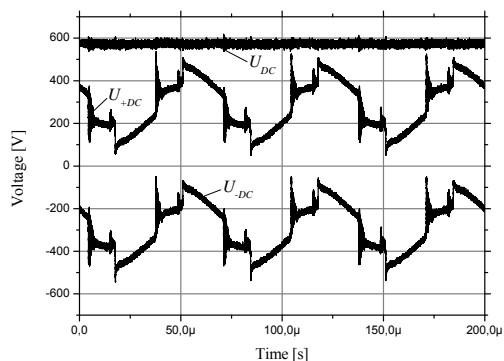


Fig. 25. DC voltage at the output of the converter (U_{DC}), plus DC-to-ground voltage ripples (U_{+DC}) and minus DC-to-ground voltage ripples (U_{-DC})

Aggregated interference introduced by group of SMCs

DC/DC converters in power systems are often connected in series or in parallel in order to provide the required electrical energy parameters. The box-and-whisker plots, presented in Fig. 26, show the distributions of one thousand average detector measurements taken in the test arrangement, comprised of five 1 kW DC/DC converters commonly used as interfaces between PV cells and a common DC bus. Each of the measurements was taken according to standard requirements, using the EMI receiver and Line Impedance Stabilization Network (LISN), in a normalized time equal to 1 s for a measuring frequency equal to the converter switching frequency.

The EMC standards require only one measurement, using a final detector (average and quasi-peak), for a given frequency. The range of the results in the case of a single operated converter (PEI 1, PEI 2, PEI 3, PEI 4, PEI 5) is lower than 1dB, but the levels of the aggregated interference, in the case of group work of two (PEI 1-2), three (PEI 1-3), four (PEI 1-4) and five (PEI 1-5) converters, differ significantly. In the presented case, for five operated PEIs (PEI 1-5), differences between single measurements

reached 17 dB. These differences result from very low frequency envelopes caused by beating between the similar switching frequencies of the operated converters.

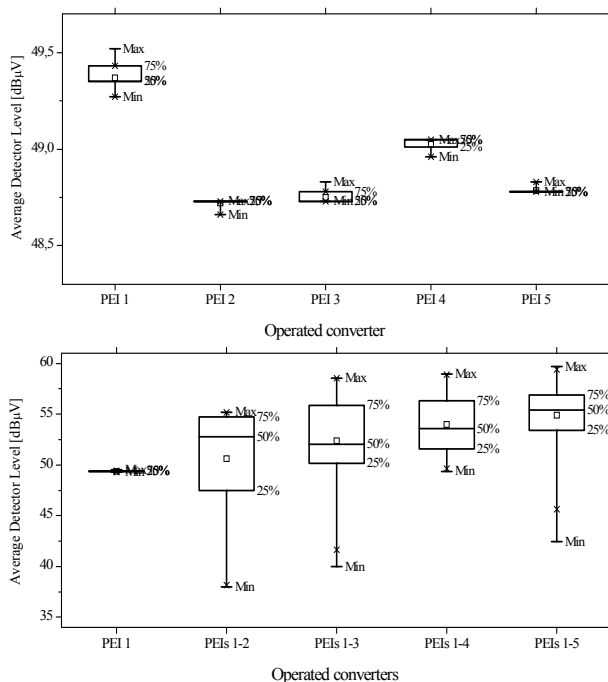


Fig. 26. Box-and-whisker plots of average detector measurements for single and multiple DC/DC converters

The obtained results showed the ineffectiveness of the normalized measuring procedures for the evaluation of the conducted EMI generated by a group of PEIs.

Conclusions

In this paper conducted high frequency disturbances introduced to electrical power systems by switch mode converters have been presented. The assurance of electromagnetic compatibility is an important factor conditioning the development of modern power systems. Typically encountered connection of susceptible control and communications electronic equipment to a high emission power electronics sector of a power system requires a special caution and in-depth EMC analysis to ensure system reliability. The selected issues accompanying application of SMCs in the power system such as the flow of interference in extensive circuits as well as aggregation of the interference caused by group of the DC/DC converters have been presented.

Magnetic field measurements have shown that interference caused by a four quadrant converter, which is widely used in various modern power system arrangements, can be transferred by parasitic couplings on the medium voltage side of the transformer.

The experimental results have shown that the aggregated interference components introduced into the electric grid by the system consisting of the same power electronic converters that individually fulfill EMC requirements might act as an incompatible unit.

REFERENCES

- [1] Hignorami N. G., Gyugi L., Understanding FACTS, *IEEE Press Series*, New York, 1999.
- [2] Song Y. H., Johns A. T., Flexible AC transmission systems (FACTS) *IEE Power Energy*, Sep. 1999, 30.
- [3] Machowski J., Elastyczne systemy przesyłowe – FACTS, *Przegląd Elektrotechniczny*, 2002, 78(7), pp. 189–96, (In Polish).

- [4] Strzelecki R., Supronowicz H., Power factor coefficient in AC power systems and their improvement method, *OW Politechniki Warszawskiej*, Warszawa 2000 (in Polish).
- [5] Sood V. K., HVDC and FACTS controllers: applications of static converters in power systems, *Springer*, London, 2004.
- [6] Benysek G., *Improvement in the quality of delivery of electrical energy using power electronics systems*, Power Systems, London, *Springer*, 2007.
- [7] Strzelecki R., Benysek G., Power electronics in smart electrical energy networks, Power Systems, London, *Springer*, 2008.
- [8] Benysek G., Strzelecki R., Modern power-electronics installations in the Polish electrical power network, *Elsevier, Renewable and Sustainable Energy Reviews*, 15 (2011), pp. 236–251.
- [9] Tenti P., Trombetti D., Tedeschi E., Mattavelli P., Compensation of load unbalance, reactive power and harmonic distortion by cooperative operation of distributed compensators, *Proc. European Power Electronics and Applications Conf. EPE 2009*, Barcelona 2009.
- [10] Akagi H., Watanabe E. H., Aredes M., Instantaneous power theory and applications to power conditioning, *IEEE Press Series on Power Engineering*, Wiley-Interscience, Piscataway, 2007.
- [11] Smoleński R., Conducted electromagnetic interference (EMI) in smart grids, London, *Springer*, 2012.
- [12] Benysek G., Kaźmierkowski M. P., Popczyk J., Strzelecki R., Power electronics systems as crucial part of smart grid infrastructure a survey. *Bull. Pol. Acad. Sci. Tech. Sci.* 59(4), 2011, pp. 455-473.
- [13] Ekanayake J., Jenkins N., Liyanage K., Wu J., Yokoyama A., Smart grid: technology and applications. *Wiley* New York 2011.
- [14] Bakran M. M., Eckel H-G., Hellsper M., Nagel A., Next Generation of IGBT-Modules Applied to High Power Traction, *Proc. European Power Electronics and Applications Conf. EPE 2007*, pp.1-9, Aalborg 2007.
- [15] Kempki A., *Conducted EMI in converter feed drive systems*, OW University of Zielona Góra, 2005 Zielona Góra (In Polish).
- [16] Konefal T., Dowson J., Denton A., Benson T., Cristopulos C., Marvin A., Porter S., Thomas D., Electromagnetic coupling between wires inside a rectangular cavity using multiple-mode-analogous-transmission-line circuit theory, *IEEE Trans. on electromagnetic compatibility*, Vol. 43 no 3, 2001, pp. 273-281.
- [17] Tarateeraseth V., EMI filter design: Part II: Measurement of noise source impedances, *Electromagnetic Compatibility Magazine*, *IEEE*, vol. 1, no. 1, pp. 42–49, 2012.
- [18] Chen W., Yang X., Wang Z., Analysis of Insertion Loss and Impedance Compatibility of Hybrid EMI Filter Based on Equivalent Circuit Model, *Industrial Electronics, IEEE Transactions on*, vol. 54, no. 4, pp. 2057–2064, 2007.
- [19] Akagi, H., Tamura S., A passive EMI filter for eliminating both bearing current and ground leakage current from an inverter-driven motor, *Power Electronics, IEEE Transactions on*, vol. 21, no. 5, pp. 1459–1469, Sep 2006.
- [20] Akagi H., Hasegawa H., Doumoto T., Design and performance of a passive EMI filter for use with a voltage-source PWM inverter having sinusoidal output voltage and zero common-mode voltage, *Power Electronics, IEEE Transactions on*, vol. 19, no. 4, pp. 1069–1076, Jul 2004.
- [21] Hartmann M., Ertl H., Kolar J., EMI filter design for a 1 MHz, 10 kW three-phase/level PWM rectifier, *Power Electronics, IEEE Transactions on*, vol. 26, no. 4, pp. 1192–1204, Apr 2011.
- [22] Smolenski R., Kempki A., Electromagnetic compatibility of four-quadrant converter drive related to its conducted emissions, *Przegląd Elektrotechniczny*, vol. 83, no. 9, pp. 79–81, 2007, Oct 2007.
- [23] Bojarski J., Smolenski R., Kempki A., Lezynski P., Pearson's random walk approach to evaluating interference generated by a group of converters, *Applied Mathematics and Computation*, vol. 219, no. 12, pp. 6437–6444, Feb 2013.
- [24] Kempki A., Strzelecki R., Smolenski R., Benysek G., Suppression of conducted EMI in four-quadrant AC drive system, in *34th Annual IEEE Power Electronics Specialists Conference*, 2003, pp. 1121–1126.
- [25] Kempki A., Strzelecki R., Smolenski R., Fedyczak Z., Bearing current path and pulse rate in PWM-inverter-fed induction motor drive, in *Power Electronics Specialists Conference, 2001. PESC. 2001 IEEE 32nd Annual*, vol. 4, 2001, pp. 2025–2030.
- [26] Smolenski R., Jarnut M., Benysek G., Kempki A., AC/DC/DC Interfaces for V2G Applications-EMC Issues, *Industrial Electronics, IEEE Transactions on*, vol. 60, no. 3, pp. 930–935, 2013.
- [27] Smolenski R., Bojarski J., Kempki A., Lezynski P., Time Domain Based Assessment of Data Transmission Error Probability in Smart Grids with Electromagnetic Interference, *Industrial Electronics, IEEE Transactions on*, PP, 2013, in press.
- [28] Holmes D. G., Lipo T. A., Pulse Width Modulation for Power Converters, *IEEE Press, Wiley Interscience*, Piscataway, 2003.
- [29] Gyugi L., Schauder C. D., Williams S. L., Rietman T. R., Torgerson D. R., Edris A., The unified power flow controller: a new approach to power transmission control, *IEEE Trans. on Power Delivery*, Vol. 10, no 2, April 1996, pp. 1085-1097.
- [30] Rusiński J., Analysis of the series-parallel active power filters in supplying networks, PhD Thesis, *University of Zielona Góra*, Zielona Góra 2005 (In Polish).
- [31] Shen W., Wang F., Boroyevich D., Liu Y., Definition and acquisition of CM and DM EMI noise for general-purpose adjustable speed motor drives, *Proceedings of the 35th IEEE Power Electronics Specialist Conference 2004*, pp.1028-1033, Aachen 2004.
- [32] Kempki A., Smoleński R., *Decomposition of EMI noise into common and differential modes in PWM inverter drive system*, *Electrical Power Quality and Utilisation. Journal* - 2006, Vol. 12, no 1, s. 53–58.
- [33] Magnusson P.C., Alexander G.C., Tripathi V.K., Weisshaar A., Transmission lines and wave propagation, *CRC Press*, 2001.
- [34] Moreira A.F., Lipo T.A., Venkataramanan G., Bernet S., High-frequency modeling for cable and induction motor overvoltage studies in long cable drives, *IEEE Transactions. on Industry Applications*, Vol. 38, No. 5, pp.1297-1306.
- [35] Kempki A., Smolenski R., Strzelecki R., Common mode current paths and their modelling in PWM inverter-fed drives, *33rd IEEE Annual Power Electronics Specialists Conference (PESC02)*, Carins, JUN, 2002.
- [36] Smoleński R., Selected conducted electromagnetic interference issues in distributed power systems, *Bulletin of the Polish Academy of Sciences: Technical Sciences*, 57(4):383–393, 2009.

Authors: dr hab. Inż. Zbigniew Fedyczak, prof. UZ, Uniwersytet Zielonogórski, Instytut Inżynierii Elektrycznej, Zakład Energoelektroniki, e-mail: Z.Fedyczak@iee.uz.zgora.pl, dr hab. inż. Adam Kempki, prof. UZ, Uniwersytet Zielonogórski, Instytut Inżynierii Elektrycznej, Zakład Elektroenergetyki, e-mail: A.Kempki@iee.uz.zgora.pl, dr hab. inż. Robert Smoleński, Uniwersytet Zielonogórski, Instytut Inżynierii Elektrycznej, Zakład Elektroenergetyki, e-mail: R.Smolenski@iee.uz.zgora.pl.